Radiographic Evaluation of Patients with Anterior Shoulder Instability

Article *in* Current Reviews in Musculoskeletal Medicine · September 2017
DOI: 10.1007/s12178-017-9433-4

4 authors, including:

Xinning Li
Boston University
104 PUBLICATIONS **867** CITATIONS

SEE PROFILE

Curr Rev Musculoskelet Med
DOI 10.1007/s12178-017-9433-4

Radiographic Evaluation of Patients with Anterior Shoulder Instability

Andrew J. Kompel[1] · **Xinning Li**[2] · **Ali Guermazi**[1] · **Akira M. Murakami**[1]

Abstract
Purpose of Review Injuries to the labrum, joint capsule (in particular the inferior glenohumeral ligament), cartilage, and glenoid periosteum are associated with anterior shoulder instability. The goal of this review is to provide common radiographic images and findings in patients with anterior shoulder instability. Furthermore, we will demonstrate the best methods for measuring anterior glenoid bone loss.
Recent Findings Magnetic resonance (MR) imaging is highly relied upon for evaluating anterior shoulder instability and can diagnose soft tissue injuries with high sensitivity. While 3D computed tomography (CT) scan has been considered the optimal tool for evaluating osseous defects, certain MR imaging sequences have been shown to have similar diagnostic accuracy. Repair of Bankart lesions is critical to stabilizing the shoulder, and in the recent years, there has been an increasing focus on imaging to accurately characterize and measure glenoid bone loss to properly indicate patients for either arthroscopic repair or anterior bony reconstruction. Furthermore, Hill-Sachs lesions are commonly seen with shoulder instability, and importance must be placed on measuring the size and depth of these lesions along with possible engagement, as these factors will dictate management.
Summary The labral-ligamentous complex and rotator cuff are primary stabilizers of the shoulder. With anterior shoulder instability, the labrum is frequently injured. MRI with an arthrogram or provocative maneuvers is the gold standard for diagnosis. Various imaging modalities and methods can be performed to identify and measure Bankart and Hill-Sachs lesions, which can then be used for surgical planning and treating shoulder instability.

Keywords Magnetic resonance imaging (MR imaging) · Arthrogram · Computed tomography (CT scan) · Anterior shoulder instability · Bankart · Hill-Sachs

Introduction

The glenohumeral joint is a complex articulation, with both static and dynamic stabilizers that allow for a wide range of motion. Injury or alteration to any number of these soft tissue or bony structures can lead to anterior joint instability. Because of this wide range of motion as well as the diversity of the critical supporting structures, imaging of the shoulder often requires a multimodality approach as well as a multiplanar approach in terms of the cross-sectional imaging. Traditionally, radiography and computed tomography (CT) have evaluated joint alignment and bony structures, while magnetic resonance (MR) imaging interpretation focused on the soft tissue structures and dynamic stabilizers. More recent improvements in MR imaging techniques have broadened the utility of MR, making these roles less defined.

The goal of this review is to discuss the various imaging modalities performed to evaluate anterior shoulder instability including radiography, computed tomography, and magnetic

This article is part of the Topical Collection on *Management of Anterior Shoulder Instability*

✉ Akira M. Murakami
Akira.Murakami@bmc.org

[1] Department of Radiology, Boston University School of Medicine, FGH Building, 820 Harrison Ave., Boston, MA 02118, USA

[2] Department of Orthopaedic Surgery, Boston University School of Medicine, 850 Harrison Avenue–Dowling 2 North, Boston, MA 02118, USA

Published online: 30 September 2017

resonance imaging. These imaging modalities are used to evaluate bony morphology and alignment as well as specific types of injuries to the labrum, joint capsule (in particular the inferior glenohumeral ligament), cartilage, and glenoid periosteum. In addition, we will review the various methods used to quantify Bankart and Hill-Sachs lesions, which can aid in treatment and surgical planning.

Osseous Injuries

Glenoid

Inferior and anterior glenoid bone defects/lesions named Bankart lesions have been proven to alter the mechanics and stability of the shoulder [1]. In addition to diagnosing the presence of a glenoid soft tissue injury, assessing the extent and size of the bone loss has implications for surgical planning [2]. It is essential for surgeons to evaluate and accurately calculate the amount of anterior glenoid bone loss to properly indicate patients for surgery between arthroscopic repair or bony procedures (Latarjet, bone grafting, etc). Shaha et al. [3••] have reported significantly worse outcomes in patients with > 13.5% glenoid bone loss after arthroscopic Bankart repair and recommended addressing these patients with either Latarjet or additional combined procedure to further stabilize the shoulder to decrease risk of recurrence.

Various methods, including calculating the glenoid width, length, and surface area, have been developed in an attempt to measure the amount of bone loss in a standardized fashion. Once a critical threshold is met for bone loss, there is a higher failure rate of arthroscopic Bankart repair; other repair options, such as a Latarjet, will be considered by the orthopedic surgeon for surgical management [1, 4].

Both CT and MRI can accurately measure glenoid bone loss, providing useful presurgical planning information. The "circle method" is the most widely used measuring technique in these modalities, utilizing surface area measurements on the sagittal view of a 2D or 3D volume-rendered CT reformat or 2D sagittal MR image of the glenoid fossa. En face, the normal inferior glenoid contour can be approximated to a true circle. Thus, the size of a Bankart lesion can be calculated by comparing the surface area of the bone defect to the expected normal surface area of the glenoid fossa as measured by the best fit circle [5, 6•, 7, 8] (Fig. 1). Sugaya et al. [5] proposed a similar measuring technique, using en face 3D CT view of the glenoid and quantifying the amount of glenoid bone loss as a percentage defect of the glenoid based on a ratio of the glenoid width against the diameter of the assumed inferior circle of the glenoid. This has also been shown to be both very reproducible and accurate in calculating bone loss. Gyftopoulos et al. [6•] recently evaluated the diagnostic accuracy of using the circle method on MRI in calculating glenoid bone loss compared to the standard 3D CT imaging. They found MRI accuracy was only 1.3% different overall when compared to the CT imaging and concluded that MRI can be an accurate alternative to 3D CT for measuring glenoid bone loss. Owens et al. [9] proposed an equation for measuring the glenoid width in both males and females for calculating glenoid bone loss. They evaluated 1264 MR images and found that glenoid width was correlated to the glenoid height measurements and that males and females were different in their respective measurements. The formula for normal glenoid width in males is (1/3 height) + 15 mm and in females is 1/3 height + 13 mm. With this standardized formula, it is possible to make accurate calculations of the amount of glenoid bone loss with only a ruler and MRI of the injured shoulder.

Humeral Head

Dislocations frequently result in a posterolateral humeral head compression fracture deformity or Hill-Sachs lesion [10](Fig. 2). These defects are generally larger than seen in chronic recurrent subluxations. Bankart lesions routinely occur simultaneously with the Hill-Sachs, and multiple

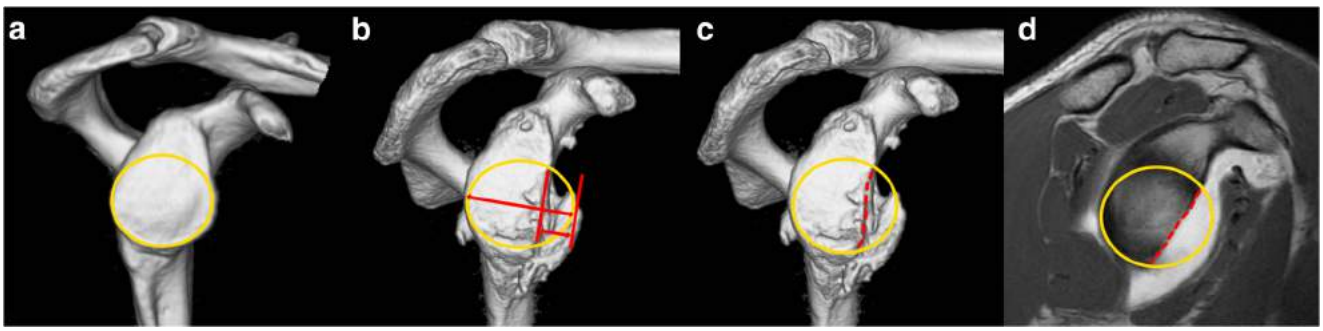

Fig. 1 Sagittal images of the glenoid estimating the size of glenoid bone loss. **a** CT volume-rendered reformat of a normal glenoid (yellow circle). **b** CT volume-rendered reformat of a bony Bankart defect measured using the Saguya method (red lines). The amount of bone loss is the ratio of the defect width against the assumed diameter of the glenoid. **c** CT volume-rendered reformat of a bony Bankart defect measured using the circle method (red outline). **d** MRI sagittal T1-weighted image of a bony Bankart defect measured using the circle method (red outline). The amount of bone loss is surface area percentage of the defect to the expected normal surface area of the glenoid

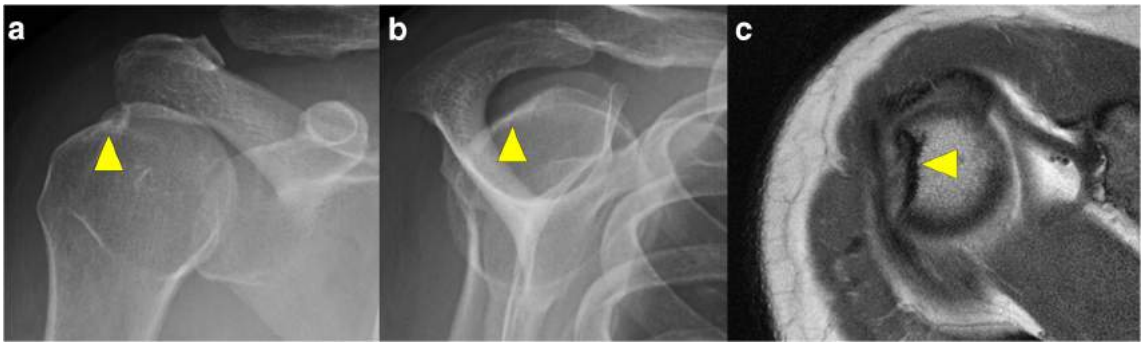

Fig. 2 Hill-Sachs lesion (arrowhead) by radiographic AP internal rotation (**a**) and scapular Y views (**b**) and MRI axial proton density (**c**)

dislocations and long-term instability can increase the size and severity of these lesions [8, 11, 12]. Studies have shown that Bankart repair can be compromised and lead to recurrent instability with a bipolar lesion when the Hill-Sachs deformity is not treated [12–18].

Similar to the Bankart lesion, a major determinate in treating a Hill-Sachs lesion is the degree of bone loss [14]. The ability to accurately quantify bone loss preoperatively can result in improved long-term shoulder stability and decreased morbidity. Multiple methods have been described in the literature based on the depth, width, and volume of the lesion. Unlike glenoid bone loss, orientation is an additional component when evaluating Hill-Sachs lesions and evaluating for potential re-engagement with the Bankart lesion [12, 19].

Various techniques in the literature using radiograph and CT to quantify Hill-Sachs lesions have been described. Kralinger et al. calculated the volume (Hill-Sachs Quotient) by measuring the length of the lesion on a Bernageau view and the width and depth on a true AP radiograph with the arm in 60° internal rotation [20]. Cho et al. demonstrated that larger Hill-Sachs lesions were more likely to engage than smaller lesions by measuring depth and width measurements on the 2DCT axial slice where the lesion is the largest [21].

Soft Tissue Injuries

Labrum and Periosteum

The anterior band of the inferior glenohumeral ligament (IGHL) commonly attaches to the anterior/anteroinferior labrum. Anterior instability leads to increased tension on the IGHL that can be transmitted to the labrum resulting in a tear or avulsion. A classic soft tissue Bankart lesion includes tearing of the labrum with a tear of the glenoid periosteum [22].

A non-displaced tear of the labrum with an intact scapular periosteum (Perthes lesion) (Fig. 3) can be a subtle finding given the potential for poor definition of the zone of chondral-labral separation. This lesion can be made more conspicuous with high-resolution MR imaging or MR arthrography. Abduction and external rotation (ABER) positioning can also can put tension on the IGHL making this injury more visible [23]. Tian et al. [24] evaluated 229 shoulder MR arthrography cases comparing the ABER position to the standard neutral position for the detection of anteroinferior labroligamentous lesions. With the ABER position, accuracy of detecting Perthes lesions was significantly better than the neutral position, 74 versus 40%, respectively.

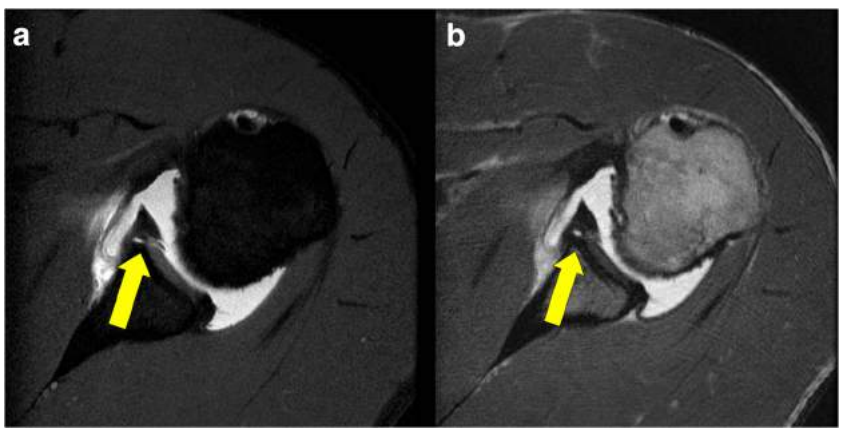

Fig. 3 Perthes lesion (arrow) on an MRI axial T1 fat saturated (**a**) and axial proton density (**b**)

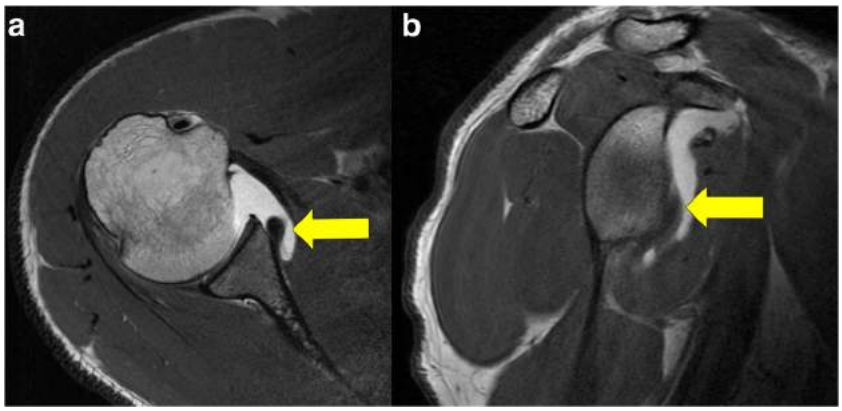

Fig. 4 Anterior labral periosteal sleeve avulsion (ALPSA) (arrow) by an MRI axial proton density (**a**) and sagittal T1 (**b**)

In cases of chronic instability, the labrum can be displaced medially onto the glenoid neck with an intact anterior scapular periosteum (ALPSA lesion) [25]. There is minimal to no anteroinferior labrum remaining in the anatomical position, and a majority of the torn labrum appears as an amorphous, hypointense structure that is medially displaced. The anterior band of the IGHL will also be displaced medially helping to identify this structure as the torn labrum and not to be confused with an intra-articular body (Fig. 4). It is important for the surgeon to recognize ALPSA lesion on both MRI and diagnostic arthroscopy to be able to mobilize this lesion off the glenoid neck and back onto the glenoid rim with the repair for successful outcomes.

Superior labral tears anterior to posterior (SLAP) can occur with multiple types of injuries and repetitive motions, presenting with non-specific symptoms. Isolated tears to the superior labrum are not common with anterior dislocations. However, anteroinferior labral tears can extend circumferentially into the superior labrum. When an anteroinferior labral tear is identified, both the axial and coronal sequences are important in describing the full extent of the tear [26, 27] (Fig. 5).

Ligaments

The IGHL is a primary stabilizer of the joint. On MR imaging, the IGHL appears as a thin (less than 4 mm) hypointense (dark) curvilinear band that is best appreciated on the oblique coronal and axial planes. With anterior shoulder instability, there is increased force on the inferior labral-ligamentous complex [4].

The anterior band of the IGHL is the most commonly torn portion. Injury can occur anywhere along the course of the complex, from the humeral to glenoid/labral attachments. Most commonly, increased tension on the IGHL leads to tearing at the labral attachment, creating the Bankart lesion. Less frequently, when the IGHL fails at the humeral attachment, the injury is called a HAGL (humeral avulsion of the IGHL). An arthrogram or joint effusion distends the joint capsule and outlines the IGHL allowing for easier identification of the injury [28, 29]. With a full-thickness tear or avulsion, fluid will extend beyond the margin of the axillary recess and into the quadrilateral space [30] (Figs. 6 and 7).

Weeks after a dislocation event, the region of hemorrhage and edema in the acutely torn IGHL will slowly be replaced by scar and granulation tissue. Although the IGHL may

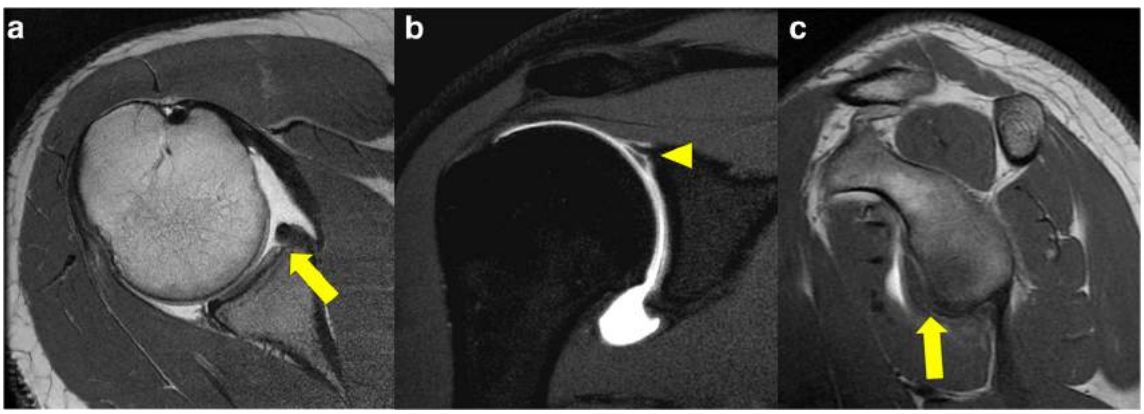

Fig. 5 Tear of the anterior-inferior labrum (arrow) with adjacent glenolabral articular disruption (GLAD) which has also extended superiorly into a tear of the superior labrum (arrow head) imaged on MRI axial proton density (**a**), coronal T1 fat saturated (**b**), and sagittal T1 (**c**)

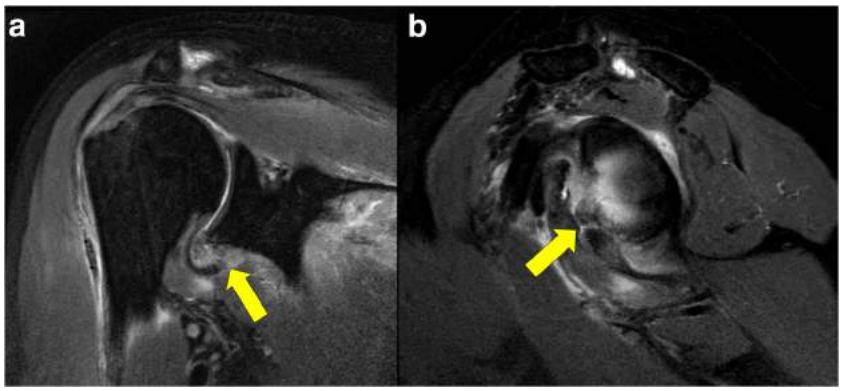

Fig. 6 Avulsion of the inferior joint capsule and anterior-inferior glenohumeral ligament from the scapular attachment (arrow) imaged on MRI coronal T2 fat saturation (**a**) and sagittal T2 fat saturation (**b**)

remain non-functional, the lower MR signal intensity of the scarring and decreased edema signal of the tissue may lead to difficulty in diagnosis.

Cartilage

The cartilage overlying the anterior-inferior glenoid can be damaged (GLAD lesion) by direct impaction of the humeral head or by tension on the cartilage from an adjacent Bankart lesion [31] (Fig. 5a). Chondral fissures and delaminations are subtle findings which can be detected by high-resolution MR imaging or MR arthrography. Over time, the chondral defect over the anterior-inferior glenoid can further increase in size due to chronic instability and secondary osteoarthritis. Additional, secondary findings which include subchondral bone marrow edema or cystic change are easily identified on MR T2 fat-suppressed sequences further outlining the overlying cartilage abnormalities [28, 32].

Rotator Cuff

The rotator cuff is a main glenohumeral joint dynamic stabilizer. Tendon tears more frequently occur in the elderly population who dislocate due to preexisting tendinosis [33]. Younger patients may have concomitant rotator cuff tendon contusions related to an acute dislocation. Evaluation with MR imaging is highly sensitive for detecting tears and early detection allows for appropriate surgical planning [34]. In older patients with cuff weakness on examination after a shoulder dislocation, an MRI is recommended to rule out acute cuff tears that may require surgical intervention.

Imaging Techniques

Traditional Radiographic Imaging

Initial presentations of shoulder instability and dislocations are imaged with radiographs. X-rays are widely available and relatively inexpensive. Radiographs provide an overview of the bony anatomy, orientation, and initial assessment for Bankart and Hill-Sachs lesions. Given the orientation of the glenohumeral joint, radiographs can be obtained relative to the body or aligned to the scapula. AP, "Y," and Grashey views are typically obtained. The AP view is aligned with the body and the "Y" and Grashey views are oriented to the scapula.

In patients who are able to abduct the arm, an axillary view is an additionally obtained view. This view is centered on the

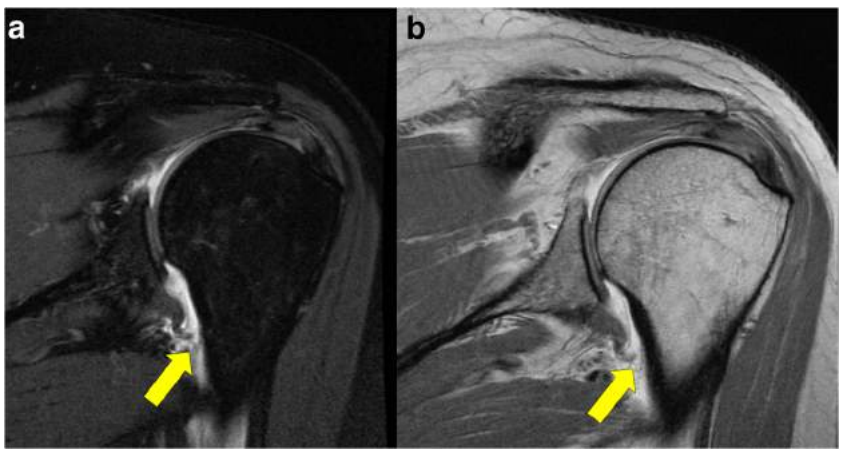

Fig. 7 Avulsion of the inferior joint capsule and anterior-inferior glenohumeral ligament from the humeral attachment (HAGL) (arrow) imaged on MRI coronal T2 fat saturation (**a**) and coronal proton density (**b**)

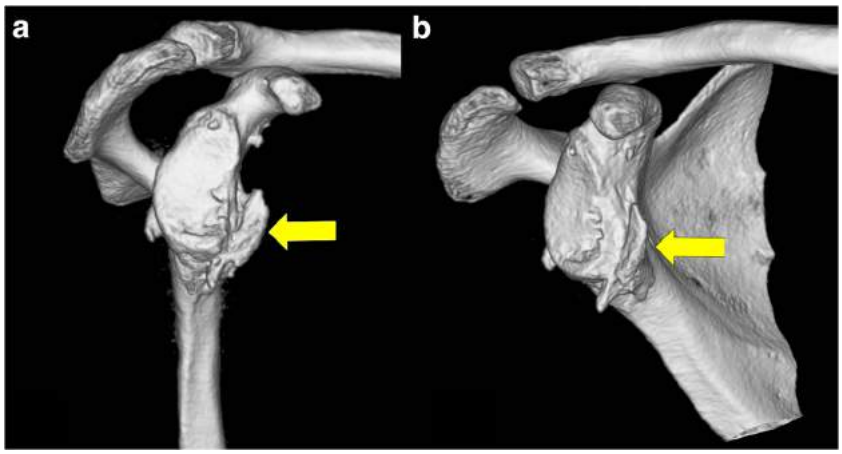

Fig. 8 CT 3D volume-rendered reformat of the shoulder with the humeral head digitally removed demonstrating a large displaced bony Bankart fragment (arrow)

epicenter of the humeral head and glenoid, and this provides an unambiguous view of anteroposterior glenohumeral alignment. Clinical concerns of anterior/posterior glenohumeral subluxation/dislocation and osseous Bankart lesions can be evaluated [35].

Less commonly performed views that can help in identifying pathology related to shoulder instability include the Valpeau, Stryker Notch, and West Point views. In patients who cannot abduct the arm, a modified axillary view (Valpeau) allows the arm to remain in a sling. The Stryker Notch and West Point views increase the detection of Hill-Sachs and Bankart lesions. For the Stryker Notch view, the patient can be standing or supine. The arm is voluntarily extended vertically with the palm placed behind the head, making the humerus parallel to the table. In the standing position, the elbow points straight in front of the patient's face, and in the supine position, it points towards the ceiling. For a West Point view, the patient is prone with the head turned away from the cassette. The forearm can hang off the table or the elbow is extended with the arm abducted 90° from the long axis of the body, resulting in the humerus parallel to the tabletop [35].

The Bernageau profile view can be used to evaluate glenoid bone loss. Ikemoto et al. described using this view to calculate the distance between the anterior and posterior glenoid rims and to compare these measurements between the left and right shoulders [36]. The Bernageau view has been shown to have similar accuracy and reproducibility as CT in detecting and measuring the degree of glenoid erosion [37]. There is also the added benefit that radiographs are cheaper, easier to perform, and available to a larger population.

CT Scan

CT has traditionally been the main diagnostic imaging modality for evaluating the bones relating to anterior shoulder instability [5]. CT scans are readily available, rapidly acquired, and provide excellent fine bony detail. Anterior shoulder dislocations can often lead to glenoid bone rim fractures (bony Bankart), and repeated subluxations can remodel the glenoid [38]. Such pathology is well imaged by CT, as the imaging can detect the smallest osseous fragments and glenoid asymmetry. When acquired with high-resolution thin slices, 3D volume-rendered reformats can also be created with the humeral head digitally removed providing further visualization of the glenoid fossa for preoperative planning and measurement or calculation of the amount of bone loss [5] (Fig. 8).

In the evaluation of Hill-Sachs lesions, CT scans with high-resolution thin slices and multi-planar reformats provide similar findings when compared to arthroscopy [19]. While isolated Hill-Sachs lesions or those associated with small Bankart lesions may be less clinically significant, bipolar lesions (Hill-Sachs and Bankart lesions occurring together) often require both arthroscopic Bankart repair and humeral head remplissage to maintain stability and minimize failure [39, 40]. If such lesions are suspected, then CT scan can accurately identify both with high precision and sensitivity.

Magnetic Resonance (MR) Imaging and MR Arthrography

MR imaging is a diagnostic tool to complement the physical exam in patients with anterior shoulder instability. One of the strengths of MR imaging is the evaluation of the soft tissues, which can be performed with high contrast and spatial resolution. In the literature, MR accuracy in identifying labral and rotator cuff tears ranges from 70 to 100% [41–43]. The acquired multiplanar imaging allows for the detailed evaluation of the glenoid, labrum, joint capsule, and rotator cuff in different planes [44].

MR arthrography refers to the MR imaging of a joint that has been injected with an intra-articular contrast agent such as diluted gadolinium or saline solution. This form of MR imaging has proven utility in detecting injuries to the labral-ligamentous complex [45]. The contrast material is injected prior to MR imaging by fluoroscopic or ultrasound guidance

under strict aseptic technique. By distending the joint capsule, the cartilage, ligaments, and labrum are outlined with contrast, increasing the sensitivity for detecting tears and other lesions [46, 47]. Similarly, a joint effusion with capsular distension seen in an acute shoulder dislocation will outline these structures, making the arthrogram unnecessary [48].

Traditionally, MR arthrography has been reserved for younger patients and athletes, where detecting subtle injuries, especially of the anterior or superior labrum may lead to changes in treatment [45]. More recently, this convention has been slightly more controversial due to a number of factors. Indeed, with improvements in shoulder coil design, software, and fast spin-echo imaging sequences, conventional 1.5-Tesla (1.5 T) MR, if done appropriately, can be acquired with a high-imaging matrix. This allows for the higher spatial resolution needed to diagnose labral-ligamentous pathology with increased sensitivity. The use of conventional 3-Tesla (3 T) MR can lead to even further improvements in image acquisition speed, signal, and spatial resolution. This provides an even higher sensitivity, specificity, and accuracy comparing well to arthroscopy, making non-arthrographic MR imaging a viable option for patients with suspected labral pathology [49, 50•, 51•].

The decision to use traditional non-contrast MR imaging versus MR arthrography should be site specific and sometimes depending on the radiologist's experience. Although MR arthrography has proven itself to be excellent at detecting labral tears in the setting of shoulder instability, imaging protocols can also vary greatly from one imaging center to another [52]. If these protocols are performed inadequately, any MR imaging sequence acquired will have decreased sensitivity regardless of the presence or absence of intra-articular contrast material. Still, with all things equal, Magee et al. [51•] demonstrated that 3-T MR arthrography had statistically significant increased sensitivity for the detection of both anterior labral tears and SLAP tears compared to the conventional 3-T MRI. These authors recommended 3-T MR arthrography as the imaging of choice for patients with shoulder instability. Either way, a close collaboration with the musculoskeletal imaging radiologist at your institution with a thorough "reason for exam" description is important and necessary to ensure that the acquired imaging sequences are adequate for the pathology being diagnosed, whether it is by arthrogram or not.

The shoulder is routinely positioned with partial external rotation for most MR scans, but various alternative positions can be used during an arthrogram which can increase the sensitivity for finding labral-ligamentous injuries. Abduction and external rotation (ABER) is a common additional position, which can increase the sensitivity for detecting anteroinferior labral-ligamentous injury [53]. However, limited range of motion or pain may prohibit patients from performing these provocative maneuvers. Schreinemachers et al. showed that full routine MR imaging or arthrogram examinations have the same accuracy as the ABER sequence in evaluating the anteroinferior labral-ligamentous complex [54].

Routinely performed MR imaging sequences are proton density (PD) and T2 fat-suppressed fast spin-echo sequences. These in particular allow for the evaluation of interstitial and bursal surface tears of the joint capsule and rotator cuff, in addition to the labrum and cartilage. These sequences also show humeral and/or glenoid bone marrow edema which may explain pain in some of these patients [55]. Non-fat-suppressed PD sequences can provide detailed anatomy of the osseous structures and is often relied upon for diagnosing subtle cortical fracture and displaced bony fragments [9, 56]. The T2 fat-suppressed sequence can also be useful in the setting of an acute osseous impaction injury, where there will be bone marrow edema (hyperintense signal) and a fracture line better seen when compared to a T1 sequence (Fig. 9). For an MR arthrogram, T1 fat-suppressed sequences in 2 or 3 planes are also performed to highlight the fine contours of the labral ligamentous structures against the hyperintense intra-articular contrast [46,47].

Recent investigations have also looked at the sensitivity of MR imaging in evaluating glenoid bone loss. As patients with anterior instability are often being scanned by MR imaging for soft tissue injuries, quantification of bone loss with the same MR images can decrease time, radiation exposure, and cost associated with obtaining an additional CT scan. Similar to

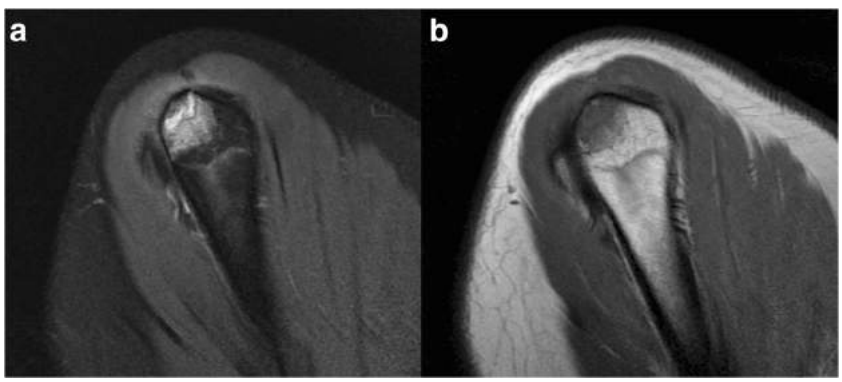

Fig. 9 Non-displaced greater tuberosity fracture on MRI sagittal T2 fat saturated (**a**) and sagittal T1-weighted sequences (**b**)

CT, 3D reconstructions of the glenoid can be created from specialized high-resolution thin slice sequences. In this setting, MR imaging can have comparable accuracy in determining the degree of bone loss [5, 6•, 7, 8].

Summary

Anterior shoulder stability primarily relies upon the labral-ligamentous complex and rotator cuff. With anterior instability and dislocations, the injury can involve the IGHL, anteroinferior labrum, adjacent glenoid cartilage, posterolateral humeral head, and glenoid rim. The labrum, along with the glenoid rim, is the most frequently damaged.

MR imaging is the gold standard, and modifications including arthrography and provocative maneuvers can increase the sensitivity for detecting these lesions. Note should also be made that MR sequences and protocols vary between institutions, and this can contribute to varied sensitivity for detecting lesions. Collaboration with the musculoskeletal radiologist is often needed to optimize the imaging protocols for proper diagnosis of these findings.

3D CT scan of the glenoid is an important companion tool for the osseous evaluation of Bankart and Hill-Sachs lesions. In particular, this modality is highly sensitive in assessing the size and location of the bone loss or bony defect. MR imaging has recently been shown to have similar accuracy for evaluation of these injuries and decreases radiation exposure, cost, and time.

Multiple methods have been described in the literature for characterizing these osseous defects. Identifying and quantifying both Bankart lesions and glenoid bone loss on imaging allow for appropriate surgical planning, which has been shown to improve patient outcome and limit recurrent instability. Hill-Sachs lesions are less commonly repaired; however, larger-size lesions that engage with the glenoid with mechanical symptoms may require surgical correction to prevent re-injury to the Bankart repair.

Compliance with Ethical Standards

Conflict of Interest Andrew J. Kompel and Akira M. Murakami declare that they have no conflict of interest.

Xinning Li is on the board of JoMI and has equity in the company. Ali Guermazi reports personal fees from BICL, LLC, Pfizer, MerckSerono, TissueGene, OrthoTrophix, Sanofi, GE, and AstraZeneca, outside of the submitted work.

Human and Animal Rights and Informed Consent This article does not contain any studies with human or animal subjects performed by any of the authors.

References

Papers of particular interest, published recently, have been highlighted as:
- • Of importance
- •• Of major importance

1. Itoi E, Lee SB, Berglund LJ, et al. The effect of a glenoid defect on anteroinferior stability of the shoulder after Bankart repair: a cadaveric study. J Bone Joint Surg Am. 2000;82:35–46.
2. Piasecki DP, Verma NN, Romeo AA, et al. Glenoid bone deficiency in recurrent anterior shoulder instability: diagnosis and management. J Am Acad Orthop Surg. 2009;17:482–93.
3. •• Shaha JS, Cook JB, Song DJ, Rowles DJ, Bottoni CR, Shaha SH, et al. Redefining "critical" bone loss in shoulder instability: functional outcomes worsen with "subcritical" bone loss. Am J Sports Med. 2015;43(7):1719–25. **Recent study illustrating the importance of accurate quantification of the amount of glenoid bone loss.**
4. Bigliani LU, Newton PM, Steinmann SP, et al. Glenoid rim lesions associated with recurrent anterior dislocation of the shoulder. Am J Sports Med. 1998;26:41–5.
5. Sugaya H. Techniques to evaluate glenoid bone loss. Curr Rev Musculoskelet Med. 2014;7:1–5.
6. • Gyftopoulos S, Hasan S, Bencardino J, et al. Diagnostic accuracy of MRI in the measurement of glenoid bone loss. AJR Am J Roentgenol. 2012;199:873–8. **Study demonstrating the accuracy of using CT measurement techniques of glenoid bone loss on sagittal MR images.**
7. Lee RK, Griffith JF, Tong MM, et al. Glenoid bone loss: assessment with MR imaging. Radiology. 2013;267:496–502.
8. Sugaya H, Moriishi J, Dohi M, et al. Glenoid rim morphology in recurrent anterior glenohumeral instability. J Bone Joint Surg Am. 2003;85-A:878–84.
9. Owens BD, Burns TC, Campbell SE, et al. Simple method of glenoid bone loss calculation using ipsilateral magnetic resonance imaging. Am J Sports Med. 2013;41:622–4.
10. Bushnell BD, Creighton RA, Herring MM. Bony instability of the shoulder. Arthroscopy. 2008;24:1061–73.
11. Yiannakopoulos CK, Mataragas E, Antonogiannakis E. A comparison of the spectrum of intra-articular lesions in acute and chronic anterior shoulder instability. Arthroscopy. 2007;23:985–90.
12. Burkhart SS, De Beer JF. Traumatic glenohumeral bone defects and their relationship to failure of arthroscopic Bankart repairs: significance of the inverted-pear glenoid and the humeral engaging Hill-Sachs lesion. Arthroscopy. 2000;16:677–94.
13. Chen AL, Hunt SA, Hawkins RJ, et al. Management of bone loss associated with recurrent anterior glenohumeral instability. Am J Sports Med. 2005;33:912–25.
14. Miniaci A, Gish M. Management of anterior glenohumeral instability associated with large Hill-Sachs defects. Tech Shoulder Elbow Surg. 2004;5:170–5.
15. Sekiya JK, Wickwire AC, Stehle JH, et al. Hill-Sachs defects and repair using osteoarticular allograft transplantation: biomechanical analysis using a joint compression model. Am J Sports Med. 2009;37:2459–66.
16. Yamamoto N, Itoi E, Abe H, et al. Contact between the glenoid and the humeral head in abduction, external rotation, and horizontal extension: a new concept of glenoid track. J Shoulder Elb Surg. 2007;16:649–56.
17. Kaar SG, Fening SD, Jones MH, et al. Effect of humeral head defect size on glenohumeral stability: a cadaveric study of simulated Hill-Sachs defects. Am J Sports Med. 2010;38:594–9.

18. Flatow EL, Warner JI. Instability of the shoulder: complex problems and failed repairs: part I. Relevant biomechanics, multidirectional instability, and severe glenoid loss. Instr Course Lect. 1998;47:97–112.
19. Sekiya J, Cutuk A. Humeral head defects—biomechanics, measurements, and treatments. In: Provencher MT, Romeo AA, editors. Shoulder instability: a comprehensive approach. Philadelphia: Elsevier Saunders; 2012. p. 234–47.
20. Kralinger FS, Golser K, Wischatta R, et al. Predicting recurrence after primary anterior shoulder dislocation. Am J Sports Med. 2002;30:116–20.
21. Cho SH, Cho NS, Rhee YG. Preoperative analysis of the Hill-Sachs lesion in anterior shoulder instability: How to predict engagement of the lesion. Am J Sports Med. 2011;39:2389–95.
22. Bankart A. The pathology and treatment of recurrent dislocation of the shouder-joint. Br J Surg. 1938;26:23–9.
23. Wischer TK, Bredella MA, Genant HK, et al. Perthes lesion (a variant of the Bankart lesion): MR imaging and MR arthrographic findings with surgical correlation. AJR Am J Roentgenol. 2002;178:233–7.
24. Tian CY, Cui GQ, Zheng ZZ, Ren AH. The added value of ABER position for the detection and classification of anteroinferior labroligamentous lesions in MR arthrography of the shoulder. Eur J Radiol. 2013;82(4):651–7.
25. Neviaser TJ. The anterior labroligamentous periosteal sleeve avulsion lesion: a cause of anterior instability of the shoulder. Arthroscopy. 1993;9:17–21.
26. Snyder SJ, Karzel RP, Del Pizzo W, et al. SLAP lesions of the shoulder. Arthroscopy. 1990;6:274–9.
27. Mohana-Borges AV, Chung CB, Resnick D. Superior labral anteroposterior tear: classification and diagnosis on MRI and MR arthrography. AJR Am J Roentgenol. 2003;181:1449–62.
28. Waldt S, Burkart A, Imhoff AB, et al. Anterior shoulder instability: accuracy of MR arthrography in the classification of anteroinferior labroligamentous injuries. Radiology. 2005;237:578–83.
29. Wolf EM, Cheng JC, Dickson K. Humeral avulsion of glenohumeral ligaments as a cause of anterior shoulder instability. Arthroscopy. 1995;11:600–7.
30. Carlson CL. The "J" sign. Radiology. 2004;232:725–6.
31. Neviaser TJ. The GLAD lesion: another cause of anterior shoulder pain. Arthroscopy. 1993;9:22–3.
32. Sanders TG, Tirman PF, Linares R, et al. The glenolabral articular disruption lesion: MR arthrography with arthroscopic correlation. AJR Am J Roentgenol. 1999;172:171–5.
33. Neviaser RJ, Neviaser TJ, Neviaser JS. Concurrent rupture of the rotator cuff and anterior dislocation of the shoulder in the older patient. J Bone Joint Surg Am. 1988;70:1308–11.
34. Morag Y, Jacobson JA, Miller B, et al. MR imaging of rotator cuff injury: what the clinician needs to know. Radiographics. 2006;26:1045–65.
35. Pavlov H, Burke M, Giesa M, et al. Orthopaedist's guide to plain film imaging. Thieme New York. 1999. p. 2–28.
36. Ikemoto RY, Nascimento LG, Bueno RS, et al. The technique to calculate glenoid bone loss with the Bernageau profile view: is it possible? Tech Shoulder Elbow Surg. 2010;11(2):37–40.
37. Murachovsky J, Bueno RS, Nascimento LG, et al. Calculating anterior glenoid bone loss using the Bernageau profile view. Skeletal Rad. 2012;41(10):1231–7.
38. Greis PE, Scuderi MG, Mohr A, et al. Glenohumeral articular contact areas and pressures following labral and osseous injury to the anteroinferior quadrant of the glenoid. J Shoulder Elb Surg. 2002;11:442–51.
39. Bollier MJ, Arciero R. Management of glenoid and humeral bone loss. Sports Med Arthrosc. 2010;18:140–8.
40. Widjaja AB, Tran A, Bailey M, et al. Correlation between Bankart and Hill-Sachs lesions in anterior shoulder dislocation. ANZ J Surg. 2006;76:436–8.
41. Roy JS, Braen C, Leblond J, et al. Diagnostic accuracy of ultrasonography, MRI and MR arthrography in the characterisation of rotator cuff disorders: a systematic review and meta-analysis. Br J Sports Med. 2015;49:1316–28.
42. Wagner SC, Schweitzer ME, Morrison WB, et al. Shoulder instability: accuracy of MR imaging performed after surgery in depicting recurrent injury—initial findings. Radiology. 2002;222:196–203.
43. Palmer WE, Brown JH, Rosenthal DI. Rotator cuff: evaluation with fat-suppressed MR arthrography. Radiology. 1993;188:683–7.
44. Patten RM, Spear RP, Richardson ML. Diagnostic performance of magnetic resonance imaging for the diagnosis of rotator cuff tears using supplemental images in the oblique sagittal plane. Investig Radiol. 1994;29:87–93.
45. Shankman S, Bencardino J, Beltran J. Glenohumeral instability: evaluation using MR arthrography of the shoulder. Skelet Radiol. 1999;28:365–82.
46. Bencardino JT, Beltran J. MR imaging of the glenohumeral ligaments. Radiol Clin N Am. 2006;44:489–502. **vii**
47. Chaipat L, Palmer WE. Shoulder magnetic resonance imaging. Clin Sports Med. 2006;25:371–86. **v**
48. Wintzell G, Haglund-Akerlind Y, Tengvar M, et al. MRI examination of the glenohumeral joint after traumatic primary anterior dislocation. A descriptive evaluation of the acute lesion and at 6-month follow-up. Knee Surg Sports Traumatol Arthrosc. 1996;4:232–6.
49. Gusmer PB, Potter HG, Schatz JA, et al. Labral injuries: accuracy of detection with unenhanced MR imaging of the shoulder. Radiology. 1996;200:519–24.
50.• Magee TH, Williams D. Sensitivity and specificity in detection of labral tears with 3.0-T MRI of the shoulder. AJR Am J Roentgenol. 2006;187:1448–52. **Study demonstrating the advantages of 3-T MRI in evaluating labral tears over 1.5-T MRI.**
51.• Magee T. 3-T MRI of the shoulder: is MR arthrography necessary? AJR Am J Roentgenol. 2009;192:86–92. **Study demonstrating the advantages of 3-T MR arthrography over non-contrast 3-T MR imaging.**
52. Subhas N, Benedick A, Obuchowski NA, et al. Comparison of a fast 5-minute shoulder MRI protocol with a standard shoulder MRI protocol: a multiinstitutional multireader study. AJR Am J Roentgenol. 2017;208:W146–W54.
53. Kwak SM, Brown RR, Trudell D, et al. Glenohumeral joint: comparison of shoulder positions at MR arthrography. Radiology. 1998;208:375–80.
54. Schreinemachers SA, van der Hulst VP, Jaap Willems W, et al. Is a single direct MR arthrography series in ABER position as accurate in detecting anteroinferior labroligamentous lesions as conventional MR arthography? Skelet Radiol. 2009;38:675–83.
55. Palmer WE, Levine SM, Dupuy DE. Knee and shoulder fractures: association of fracture detection and marrow edema on MR images with mechanism of injury. Radiology. 1997;204:395–401.
56. Huijsmans PE, Haen PS, Kidd M, et al. Quantification of a glenoid defect with three-dimensional computed tomography and magnetic resonance imaging: a cadaveric study. J Shoulder Elb Surg. 2007;16:803–9.